

SIMULATION OF BIDIRECTIONAL BUCK BOOST DC-DC CONVERTER FOR INDUCTION MOTOR BASED ELECTRIC VEHICLE APPLICATION.

MANDADI SAGAR REDDY¹, Asst.Prof D.POMYA²

Department of Electrical and Electronics Engineering,

Anurag Engineering College,

Kodad, Nalgonda(Dist), Telangana, India

¹msreddy217@gmail.com

²pomya.naik@gmail.com

Abstract--- In this paper a universal Power Interface for all the above discussed type of vehicles. Basically, the proposed converter interfaces the energy storage device of the Electric Vehicle with the motor drive and the external charger. The proposed converter is capable of operating in all directions in buck or boost modes with a non inverted output voltage (positive output voltage with respect to the input) and bidirectional power flow. In extension to the work the proposed Power Interface is Fed to a Induction Motor Drive and the performance is analyzed.

Keywords- bidirectional, buck boost, dc link

I.INTRODUCTION

ELECTRIFICATION of the transportation industry is essential due to the improvements in higher fuel economy, better performance, and lower emissions [1]–[6]. In vehicular applications, power electronic dc/dc converters require high power bidirectional flow capability with wide input range since the terminal voltage of energy storage devices varies with the state of charge (SoC) and load variations [7]. In the case of hybrid electric vehicle(HEV), a bidirectional dc/dc converter interfaces the energy storage device with the motor drive inverter of the traction machine; i.e., the converter is placed between the battery and the high-voltage dc bus. In acceleration or cruising mode, it should deliver power from the battery to the dc link, whereas in regenerative mode, it should deliver power from the dc link to the battery. In the case of an EV or plug-in hybrid electric vehicle (PHEV), while accomplishing the aforementioned task, the bidirectional dc/dc converter also interfaces the battery with the ac/dc converter during charging/discharging from/to grid [8]. Therefore, the bidirectional dc/dc converter should interface the battery with the charging converter, as well. Fig.1 illustrates the role of the bidirectional dc/dc converter in the electrical power system of a plug-in electric vehicle [9].

In grid-connected mode, the bidirectional dc/dc converter must have the capability to convert the output voltage of the ac/dc converter into a suitable voltage to recharge the batteries and vice versa when injecting power to

the grid. In driving mode ,dc/dc converter should be able to regulate the dc link voltage for wide range of input voltages. In driving mode, usually the battery voltage is stepped-up during acceleration. DC link voltage is stepped-down during braking, where $V_{dc} > V_{batt}$. However, if motor drive's nominal voltage is less than battery's nominal voltage, $V_{dc} < V_{batt}$, the battery voltage should be stepped-down during acceleration and the dc link voltage should be stepped up during regenerative braking. In addition to these cases, in an HEV to PHEV conversion, the grid interface converter's output voltage might be less or more than the battery's nominal voltage [10], depending on the grid's V_{ac} voltage and the grid interface converter's topology. The rectified grid voltage should be stepped-up if $V_{rec} < V_{batt}$ in V2G charging mode or the battery voltage should be stepped-up for V2G discharging mode. If the rectified grid voltage is more than the battery's nominal voltage, i.e., $V_{rec} > V_{batt}$, the rectified voltage should be stepped-down in V2G charging mode and the battery voltage should be stepped-up in V2G discharging mode.

When all these possibilities are considered, the need for a universal bidirectional dc/dc converter is obvious which should be capable of operating in all-

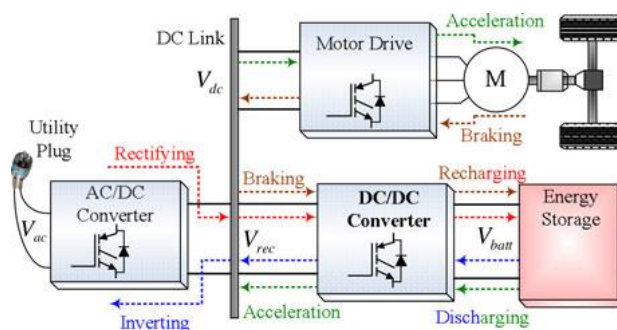


Fig. 1. Power electronic interfaces in an electric vehicle.

directions with stepping-up and stepping-down functionalities. Such a universal converter would meet all the needs of the auto industry. The proposed converter in this manuscript not only fulfills these conditions, but also can be utilized for retrofit conversion of conventional cars to HEVs as well as the HEV to PHEV conversions. It can be placed between the energy storage device and the high-voltage bus of the vehicle regardless of the nominal voltage.

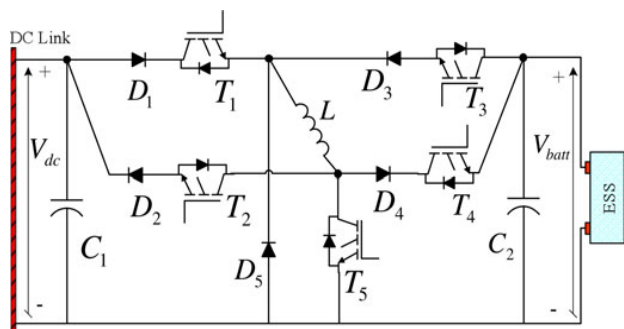


Fig. 2. Proposed fully directional universal dc/dc converter.

ratings of the battery, motor drive, and the grid interface converter inputs and outputs. Therefore, the proposed converter is called a fully directional converter. This paper is organized as follows. In Section II, the topological overview and the operation modes are presented. The analytical model of the converter and the control system development is given in Section III. Section IV focuses on the simulation and experimental results to evaluate and validate the capabilities of the proposed converter. Finally, the conclusion remarks and future work are provided in Section V.

II. SYSTEM DESCRIPTION AND OPERATING MODES

The circuit schematic of the proposed converter is depicted in Fig. 2. The converter has five power switches (T_1 – T_5) with internal diodes and five power diodes (D_1 – D_5), which are going to be properly combined to select buck and boost modes of operation. Here, V_{dc} represents the motor drive nominal input voltage during driving mode or the rectified ac voltage at the output of the grid interface converter during plug-in mode (also the input voltage of the grid interface converter to be inverted to ac). The nominal voltage of the vehicle's ESS is represented by V_{batt} . The proposed converter is capable of operating from V_{dc} to V_{batt} boosting, V_{dc} to V_{batt} bucking, V_{batt} to V_{dc} boosting, or V_{batt} to V_{dc} bucking, all with positive output voltage. In any of the four modes, only one of the power switches is operated in pulse width modulation (PWM) mode, while all the others are completely ON or OFF. Therefore, the switching losses are not more than that of any conventional buck or boost converter. In addition, the proposed converter requires only one high-current inductor unlike some of the existing buck and boost converter combinations or the cascaded configurations.

Conventional buck–boost converters can step-up or step-down the input voltage. However, they are not capable of providing bidirectional power flow. Moreover, their output voltage is negative with respect to the input voltage, which needs an inverting transformer to make the output voltage positive [11]. The non-inverted operation capability of the proposed converter totally eliminates the need for an inverting transformer, which reduces the overall size and cost. Although there are some non-inverted topologies [12]–[22], some of them require two or more switches being operated in PWM mode that causes higher total switching losses [12]–[14], [16]–[23].

TABLE I
OPERATION MODES OF THE PROPOSED CONVERTER

Direction	Mode	T_1	T_2	T_3	T_4	T_5
$V_{dc} \rightarrow V_{batt}$	BOOST	ON	OFF	OFF	ON	PWM
$V_{dc} \rightarrow V_{batt}$	BUCK	PWM	OFF	OFF	ON	OFF
$V_{batt} \rightarrow V_{dc}$	BOOST	OFF	ON	ON	OFF	PWM
$V_{batt} \rightarrow V_{dc}$	BUCK	OFF	ON	PWM	OFF	OFF

Among these topologies, although they provide buck or boost operations, bidirectional power flow cannot be achieved in the topologies of [12], [16], [19], and [24]–[26]. The conventional two-quadrant bidirectional converters would operate buck mode in one direction and boost mode in the other direction; however, they cannot operate vice versa. They would not step-up the voltage in the direction that they can step-down [15], [18], [27], [28]. Two cascaded two-quadrant bidirectional converters may achieve bidirectional power flow with bucking or boosting capabilities; however, they require more than one high-current inductor [13], [17]. In [18], although two switches and two inductors are used, only unidirectional bucking or boosting can be achieved. In the case of a dual-active bridge dc/dc converter, all switches are operated in PWM mode; therefore, switching losses are four times higher in the half-bridge case or eight times higher in full-bridge case than that of the proposed converter. Dual-active bridge dc/dc converters [29]–[41] also require a transformer at the middle stage which would increase the overall losses, size, and cost [20]–[23]. In [20], two inductors are required in addition to the transformer, and in [21] the number of inductors is three. In [22], bidirectional power flow is possible with ten switches and two inductors. Although soft switching strategies can be considered for dual-active bridge dc/dc converters in order to reduce the switching losses such as in [23], there should be eight power switches and eight power diodes with three inductors; therefore, a high number of components would not be economical. Moreover, having more than one switch operating in PWM mode would make the control system more complicated. However, in the proposed converter, the controls are as simple as the conventional buck or boost dc/dc converters in spite of all the competences. Finally, in [24], the proposed dc/dc converter requires two transformers with one being multi-winded which complicates the structure, adds up to cost, and it does not have the bidirectional operating

capability. The operation capabilities of the proposed converter significantly increases the flexibility of the converter while offering a broad range of application areas in all HEV and PHEV applications as well as their conventional to HEV or HEV to PHEV conversions with add-on batteries regardless of the voltage ratings of the motor drive, battery, and the grid interface converter. The different operation modes of the converter, including the status of the corresponding switches in each mode and the direction of power flow, are mapped in Table I. T_2 and T_4 serve as simple ON/OFF switches to connect or disconnect the corresponding current flow paths, whereas T_1 , T_3 , and T_5 are either ON/OFF or PWM switches with respect to the corresponding operating mode. Different cases and operating modes of the converter are detailed in following sections.

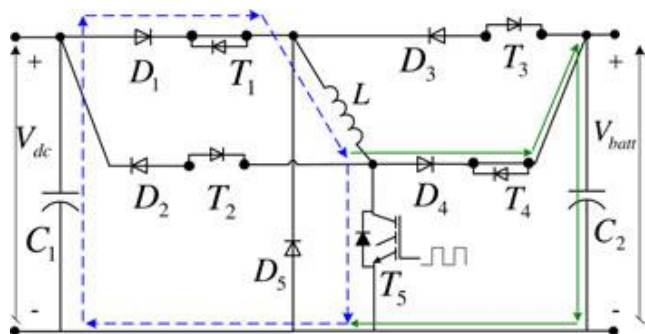


Fig. 3. V_{dc} -to- V_{batt} boost mode of operation.

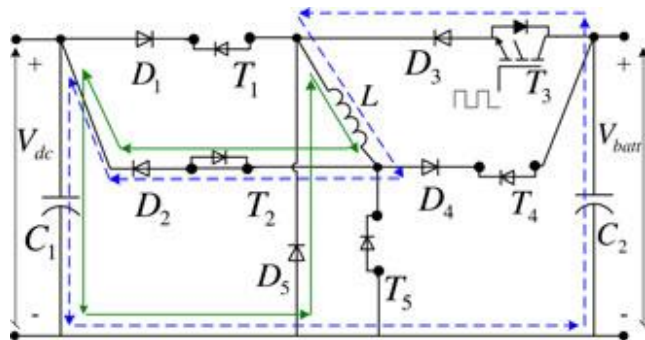


Fig. 4. V_{batt} -to- V_{dc} buck mode of operation.

A. Case 1: $V_{dc} < V_{batt}$

If the rated dc link voltage is less than battery's rated voltage, the dc link voltage should be stepped-up during charging in grid connected mode and in regenerative braking during driving. Under the same voltage condition, the battery voltage should be stepped-down during plug-in discharging in grid-connected mode, and in acceleration or cruising during driving.

Mode 1) $V_{dc} \rightarrow V_{batt}$ Boost Mode for Plug-in Charging and Regenerative Braking:

In this mode, T_1 and T_4 are kept ON, while T_2 and T_3 remain in the OFF state, as shown in Fig. 3. The PWM switching signals are applied to switch T_5 . Therefore, from V_{dc} to V_{batt} , a boost converter is formed by D_1 , T_1 , L , T_5 , D_4 , and T_4 . Since D_1 and D_4 are forward-biased, they conduct; whereas D_3 and D_2 do not conduct. Since T_5 is in PWM switching mode, when it is turned ON, the current from V_{dc} flows through D_1 , T_1 , L , and T_5 while energizing the inductor. When T_5 is OFF, both the source and the inductor currents flow to the battery side through D_4 and T_4 .

During this mode, V_{dc} and V_{batt} sequentially become the input and output voltages. Since the inductor current is a state variable of this converter, it is controllable. Therefore, the charging power delivered to the battery in plug-in mode or high-voltage bus current in regenerative braking can be controlled.

Mode 2) $V_{batt} \rightarrow V_{dc}$ Buck Mode for Plug-in Discharging and Acceleration:

The circuit schematic of this operation mode is provided in Fig. 4. In this mode, T_1 , T_4 , and T_5 remain OFF, while T_2 is kept in ON state all the time. The PWM switching signals are applied to switch T_3 . Therefore, from V_{batt} to V_{dc} , a buck converter is formed by T_3 , D_3 , D_5 , L , T_2 , and D_2 . When T_3 is turned ON, the current from the battery passes through T_3 , D_3 , L , T_2 , and D_2 while energizing the inductor. When T_3 is OFF, the output current is freewheeled through the D_5 , T_2 , and D_2 , decreasing the average current transferred to the load.

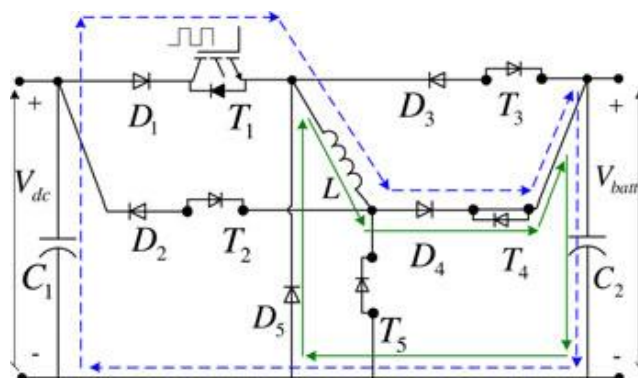


Fig. 5. V_{dc} -to- V_{batt} buck mode of operation.

side. D_3 and D_2 are forward-biased, whereas D_1 and D_4 do not conduct. D_5 only conducts when T_3 is OFF. In this mode, V_{batt} and V_{dc} are the input and output voltages, respectively. During stepping-down the battery voltage while delivering power from battery to the dc link, the inductor is at the output and its current is a state variable. Therefore, the dc link voltage and the current delivered to the dc link can be controlled in driving mode.

B. Case 2: $V_{dc} > V_{batt}$

If the rated dc link voltage is more than the battery's rated voltage, dc link voltage should be stepped-down during charging in grid-connected mode and in regenerative braking while the vehicle is being driven. Under the same voltage condition, the battery voltage should be stepped-up during plug-in discharging in grid-connected mode and in acceleration or cruising while driving.

Mode 3) $V_{dc} \rightarrow V_{batt}$ Buck Mode for Plug-in Charging and Regenerative Braking:

In this mode, T_1 is in the PWM switching mode. Switches T_2, T_3 , and T_5 remain in OFF state while T_4 is kept ON all the time. Therefore, from V_{dc} to V_{batt} , a buck converter is made up by D_1, T_1, D_5, L, D_4 , and T_4 as shown in Fig. 5. When T_1 is turned ON, the current from V_{dc} passes through D_1, T_1, L, D_4 , and T_4 while energizing the inductor. When T_1 is OFF, the output current is recovered by freewheeling diode D_5 decreasing the average current transferred from dc link to the battery. Since diodes D_1 and D_4 are forward biased, they conduct whereas D_2 and D_3 do not conduct. D_5 only conducts when T_1 is OFF. In this mode, V_{dc} and V_{batt} are the input and output voltages, respectively. The dc link voltage can be regulated in driving mode (regenerative braking) by controlling the current transferred to the battery. In plug-in charging mode, the current or power delivered to the battery is also controllable.

Mode 4) $V_{batt} \rightarrow V_{dc}$ Boost Mode for Plug-in Discharging and Acceleration:

During this mode, T_1 and T_4 remain OFF, whereas T_2 and T_3 remain ON all the time. Switch T_5 is operated in PWM switching mode. Therefore, from V_{batt} to V_{dc} , a boost converter is formed by T_3, D_3, L, T_5, T_2 , and D_2 as illustrated in Fig. 6. When T_5 is turned ON, the current from V_{batt} passes through T_3, D_3, L , and T_5 while energizing the inductor. When T_5 is OFF, both inductor and the source currents pass through T_2 and D_2 to the dc link. In this mode, D_3 and D_2 are forward-biased and they conduct, whereas

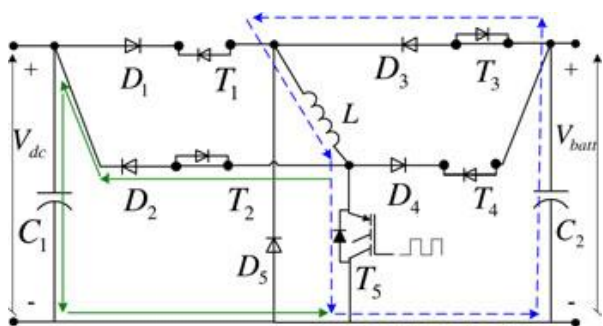


Fig. 6. V_{batt} -to- V_{dc} boost mode of operation.

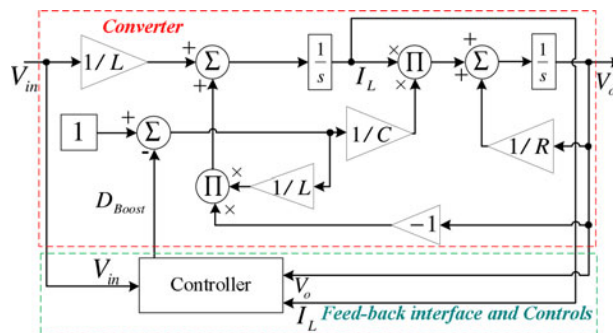


Fig. 7.

State-space model of the simplified converter in boost mode.

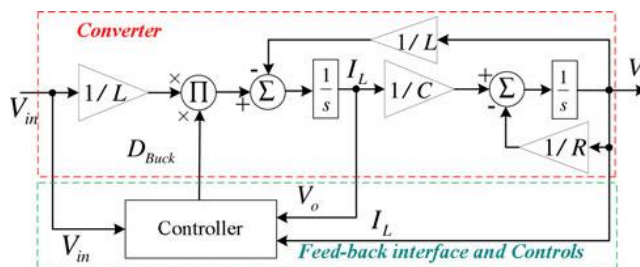


Fig. 8. State-space model of the simplified converter in buck mode.

D_1, D_4 , and D_5 are reverse-biased and do not conduct. In this mode, V_{batt} and V_{dc} are sequentially the input and output voltages. The dc link voltage can be regulated in driving mode (regenerative braking) by controlling the current drawn from the battery. In plug-in charging mode, the current or power drawn from battery is also controllable.

III. CONTROL SYSTEMS

For the control system of the proposed topology, an all electric range focused operating strategy has been considered [25]. As described in Section II and shown in Figs. 3–6, all operation modes of the proposed converter are combinations of buck and boost operations with different configurations and input/output voltages, as expressed in Table I. Therefore, simplified state-space averaged large-signal transfer functions of the buck or boost modes of operations can be derived. The state space block diagrams for the boost and buck modes of operations of the proposed converter are shown in Figs. 7 and 8. Two different controllers are incorporated for the proposed system: one employed in plug-in charging/discharging and the other is for acceleration/deceleration during driving. In plug-in

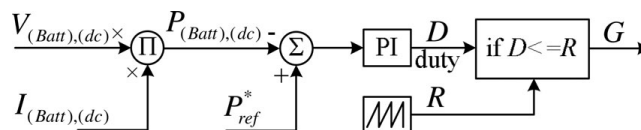


Fig. 9. DC/DC converter charge/discharge power controller.

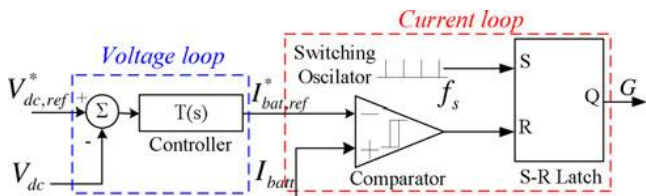


Fig. 10. DC/DC converter's cascaded controller for driving mode.

TABLE II
EXPERIMENTAL CONDITIONS AND CIRCUIT PARAMETERS

Experimental Conditions	
Reference DC link voltage	$V_{dc} = 24 \text{ or } 42 \text{ V}$
Battery terminal voltage	$V_{batt} = 42 \text{ or } 24 \text{ V}$
Switching frequency	$f_s = 20 \text{ kHz}$
Controls execution time	$T_{sc} = 20 \mu\text{s}$
Battery type	547-PS Power-Sonic sealed lead acid
DSP module	TI-TMS320F2812
Circuit Parameters	
L	3 mH
$C_{dc}=C_{batt}$	2200 μF
Power Switches	HGTG30N60A4D IGBT
Diodes	FFPF30U60STTU
Voltage Sensor	LV 20-P
Current Sensor	LA 100-P

mode, generally, it is desired to control the charging or discharging power of the battery, whereas in driving mode it is important to provide a regulated dc link voltage to the motor drive. Therefore, a power controller is used for plug-in modes and a double-loop voltage and current controller is employed for acceleration/braking modes of the driving. The battery power controller, shown in Fig. 9, allows the reference charge or discharge power to/from the battery to be tracked. This reference power can be determined based on the SoC of the battery, user requirements, and the state of the grid. The cascaded voltage and current controller, shown in Fig. 10, allows the high-voltage bus to be kept at the proper voltage while also accommodating the power demanded or supplied by the dc link. This enables regenerative recharging of the battery from the dc link and discharging of the battery to the dc link, while maintaining the proper dc link voltage level for the hybrid vehicle.

IV. EXPERIMENTAL SETUP, RESULTS, AND DISCUSSIONS

The details of the experimental setup of the proposed converter are provided in Table II. Since the proposed topology is new and has not been built or tested before, it is more appropriate to build the small-scale prototypes rather than the full-scale high power converters. Moreover, due to the safety purposes and to protect the students and the laboratory equipment, a smaller scale prototype with lower voltage rating is preferred to serve as a proof of principle.

For the experimental tests, in each mode, voltage

is applied to one terminal, representing the charging voltage or regenerative braking while output is a load, representing the battery charging load or regenerative braking power of the motor drive. In the other mode, battery is the source while the dc link is thload, representing the plug-in discharging or acceleration mode.

A. Case 1. Mode 1: $V_{dc} \rightarrow V_{batt}$ Boost

The experimental results for this mode of operation are presented in Fig. 12 where channel 1 is V_{dc} , channel 2 is V_{batt} , channel 3 is input current before the capacitor, and channel 4 is the switching signal of switch T5. As shown in Fig. 12, 24-V V_{dc} voltage is boosted to slightly more than the 42 V, battery rated voltage V_{batt} .

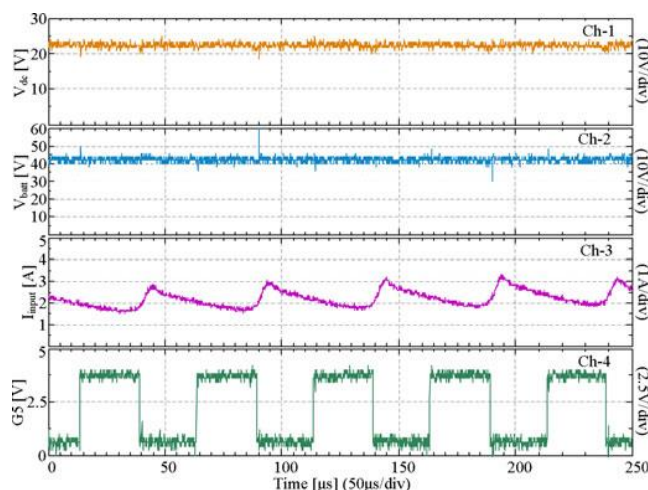


Fig. 12. Experimental results for V_{dc} -to- V_{batt} boost mode.

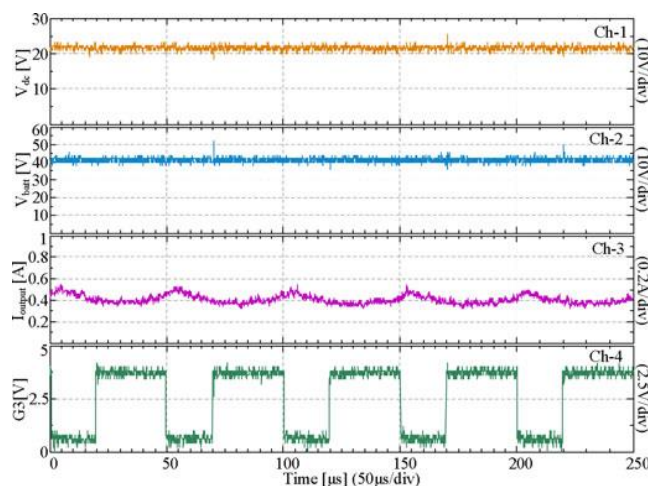


Fig. 13. Experimental results for V_{batt} -to- V_{dc} buck mode.

B. Case 1. Mode 2: $V_{batt} \rightarrow V_{dc}$ Buck

The experimental results for this mode of operation are presented in Fig. 13, where channel 1 is V_{dc} , channel 2 is V_{batt} , channel 3 is output current after the capacitor, and channel 4 is the switching signal of switch T3. The input voltage V_{batt}

is stepped-down to about 24 V (V_{dc} terminals), as shown in Fig. 13.

C. Case 2, Mode 3: $V_{dc} \rightarrow V_{batt}$ Buck

The experimental results for this mode of operation are presented in Fig. 14 where channel 1 is V_{dc} , channel 2 is V_{batt} , channel 3 is output current after the capacitor, and channel 4 is the switching signals of the switch $T1$. From Fig. 14, it is seen that the input voltage of V_{dc} is stepped down to 24 V of the battery terminal voltage.

D. Case 2, Mode 4: $V_{batt} \rightarrow V_{dc}$ Boost

The experimental results for this mode of operation are presented in Fig. 15, where channel 1 is V_{dc} , channel 2 is V_{batt} ,

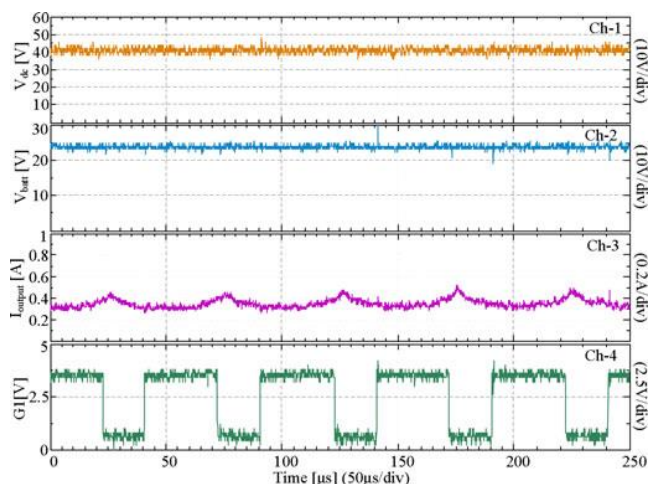


Fig. 14. Experimental results for V_{dc} -to- V_{batt} buck mode.

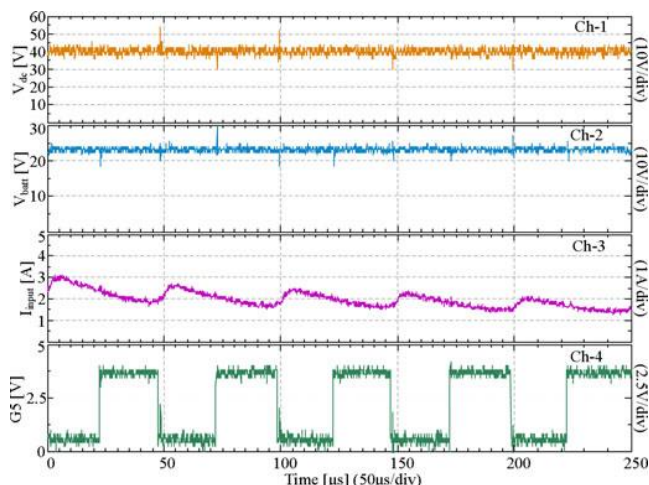


Fig. 15. Experimental results for V_{batt} -to- V_{dc} boost mode.

channel 3 is input current before the capacitor, and channel 4 is the switching signal of switch $T5$. It can be seen from Fig.

15 that the modified converter is capable of boosting the 24 V of V_{batt} voltage to about 42 V of V_{dc} output voltage.

The capacitors at the input and output of the converter, $C_{dc} = C_{batt} = 2200 \mu F$, possess a portion of energy stored at the input and output of the converter; therefore, the input or output currents of the proposed topology are not necessarily equal to the inductor current. For boost modes of operation, the input currents and for the buck modes of operations the output currents are presented in the results.

In order to present the long-term performance of the proposed converter over a drive cycle and to show the capability of switching between the modes for each of the cases, simulations were performed in addition to the experiments. For the simulations, a portion of Urban Dynamometer Driving Schedule drive cycle has been implemented that includes driving conditions such as acceleration, braking, and idling. In order to make an accurate analysis, the simulations were also down scaled assuming a rated dc link voltage of 24 V and rated battery voltage of

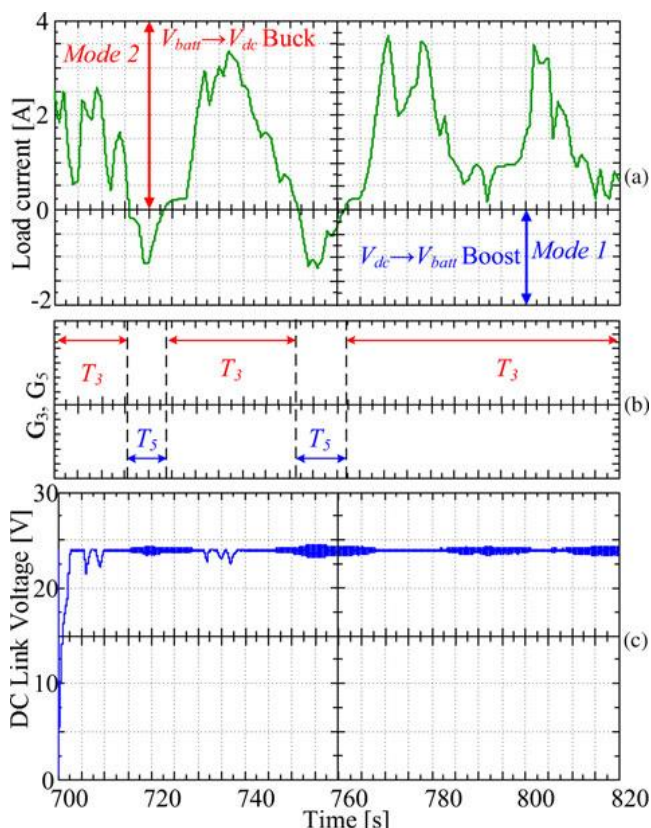


Fig. 16. Simulation results for Case 1, Modes 1 and 2. (a) Load current and switching between respective modes. (b) Switches in PWM mode with respect to the operating mode. (c) Regulated load bus voltage.

42 V for Case 1, and assuming a rated load bus voltage of 42 V and rated battery voltage of 24 V for Case 2, respectively. The load demand of the drive cycle is also scaled-down, keeping the same load demand profile. Simulation results for Case 1 are presented in Fig. 16. In Fig. 16(a), the load current

that corresponds to the load demand of the drive cycle is presented. When the load demand is positive (*Mode 2*), the vehicle is accelerating and battery power should be delivered to the dc link. Since $V_{dc} < V_{batt}$, battery voltage should be stepped-down in this situation. When the load demand is negative (*Mode 1*), motor drive delivers power from the traction machine to the dc link. Therefore, power should be recovered from the dc link to the battery by stepping-up the dc link voltage and supplying the braking energy to the battery. The switches receiving PWM signals are mapped in Fig. 16(b) with respect to the operation mode. Finally, regulated dc link voltage at 42 V is presented in Fig. 16(c).

Simulation results for *Case 2* are presented in Fig. 17 under the same load conditions. In Fig. 17(a), the load current that corresponds to the load demand of the drive cycle is presented. When the load demand is Positive (*Mode 4*), the vehicle is accelerating and battery power should be delivered to the dc link. Since $V_{dc} < V_{batt}$, the battery voltage is boosted in this situation. When the load demand is negative (*Mode 3*), the vehicle is being braked and the motor drive delivers power from traction machine to the dc link. Therefore, power should be recovered from the dc link to the battery by stepping-down the dc link.

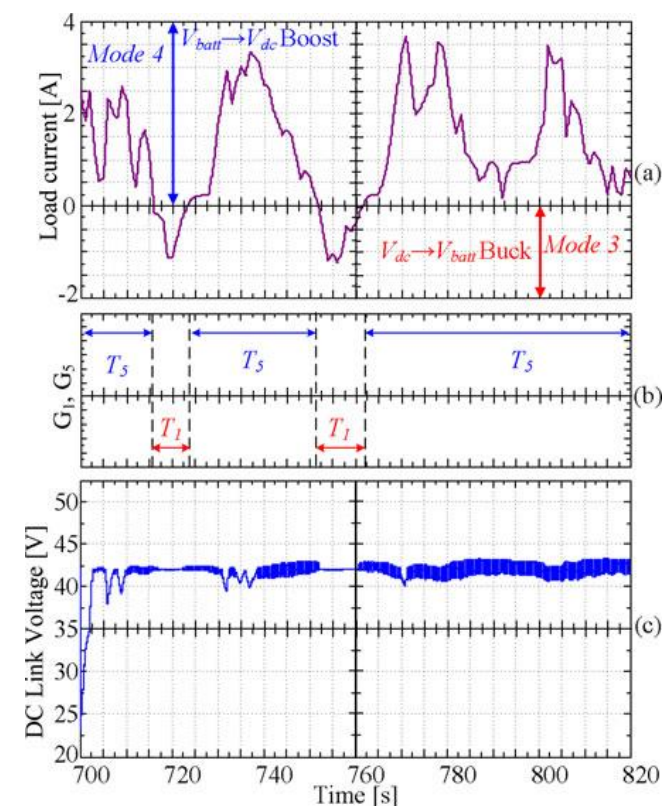


Fig. 17. Simulation results for Case 2, Modes 2 and 3. (a) Load current and switching between respective modes. (b) Switches in PWM mode with respect to the operating mode. (c) Regulated load bus voltage

The switches receiving PWM signals are mapped in Fig. 17(b) with respect to the mode of operation. Finally,

regulated dc link voltage at 24 V is presented in Fig. 17(c). In both Figs. 16 and 17, converter switches from buck to boost or boost to buck modes of operation as the load current changes its direction. In all cases, converter performs well and the dc link voltage is not affected by these changes as it is regulated continuously. The transition from acceleration to/from regenerative braking does not affect the converter's stability as well.

V. EXTENSION

Basically, the proposed converter interfaces the energy storage device of the vehicle with the motor drive and the external charger, in case of PHEVs. The proposed converter is capable of operating in all directions in buck or boost modes with a non inverted output voltage (positive output voltage with respect to the input) and bidirectional power flow. In extension to the work the proposed Power Interface is Fed to a Induction Motor Drive and the performance is analyzed.

The following figures 18,19,20 are simulation results for Induction Motor Drive.

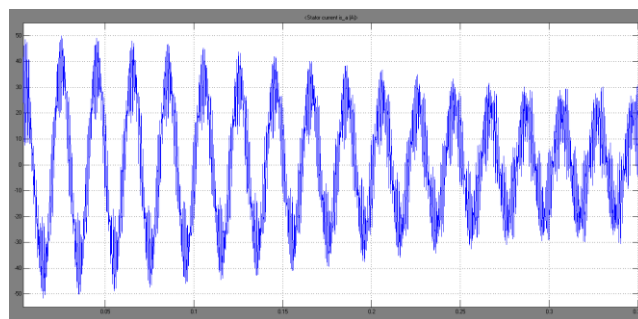


Fig: 18 shows the stator current.

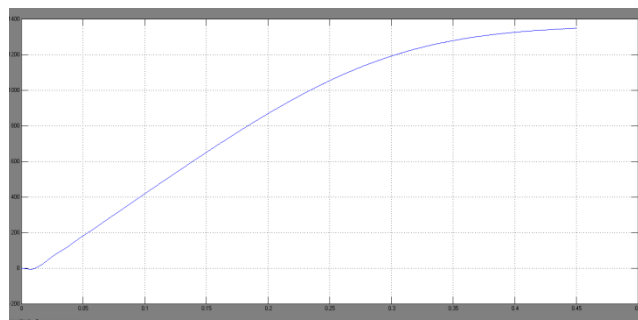


Fig: 19: shows the rotor speed.

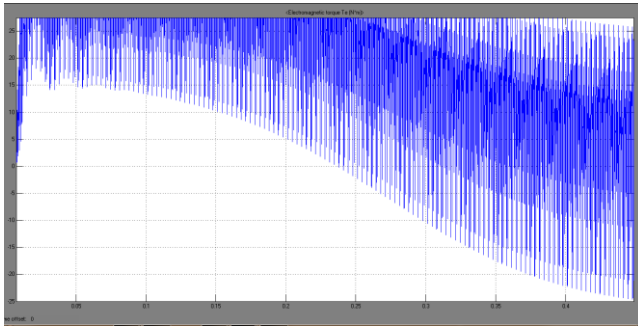


Fig: 4.5: shows the Electromagnetic torque.

VI.CONCLUSION

This study presents a novel dc/dc converter structure that is suitable for both industrial needs and the retrofit electric and vehicle conversion approaches for all EV, HEV, PHEVs regardless of their rated dc link voltage and motor drive inverter voltage as well as the battery nominal voltage. The functionalities of the proposed converter provide a broad range of application areas. Due to the operational capabilities, the proposed converter is one of a kind plug-and-play universal dc/dc converter that is suitable for all electric vehicle applications. The proposed topology is suitable not only for conversion approaches but also is a good candidate to reduce the number of dc/dc converters from two to one in commercially available vehicles such as Toyota Prius., the functionalities for two different cases with four different modes have been verified. In each case, bidirectional power flow is provided with fully directional bucking and boosting capabilities.

REFERENCES

- 1 A. Emadi, Y. L. Lee, and R. Rajashekara, "Power electronics and motor drives in electric, hybrid electric, and plug-in hybrid electric vehicles," *IEEE Trans. Ind. Electron.*, vol. 55, no. 6, pp. 2237–2245, Jun. 2008.
- 2 R. Ghorbani, E. Bibeau, and S. Filizadeh, "On conversion of electric vehicles to plug-in," *IEEE Trans. Veh. Technol.*, vol. 59, no. 4, pp. 2016–2020, May 2010.
- 3 F. H. Khan, L. M. Tolbert, and W. E. Webb, "Bi-directional power management and fault tolerant feature in a 5-kW multilevel dc-dc converter with modular architecture," *IET Power Electron.*, vol. 2, no. 5, pp. 595–604, 2009.
- 4 G. Zorpette, "The smart hybrid," *IEEE Spectrum*, vol. 41, no. 1, pp. 44–47, Jan. 2004.
- 5 Energy Independence and Security Act of 2007 (CLEAN Energy Act of 2007), *One Hundred Tenth Congress of the United States of America*, At the First Session, Washington DC Jan. 2007.
- 6 Z. Amjadi and S. S. Williamson, "Power-electronics-based solutions for plug-in hybrid electric vehicle energy storage and management systems," *IEEE Trans. Ind. Electron.*, vol. 57, no. 2, pp. 608–616, Feb. 2010.
- 7 S. Han and D. Divan, "Bi-directional DC/DC converters for plug-in hybrid electric vehicle (PHEV) applications," in *Proc. 23rd Annu. IEEE Appl. Power Electron. Conf. Expo.*, Austin, TX, Feb. 2008, pp. 787–789.
- 8 D. C. Erb, O. C. Onar, and A. Khaligh, "Bi-directional charging topologies for plug-in hybrid electric vehicles," in *Proc. 25th Annu. IEEE Appl. Power Electron. Conf. Expo.*, Palm Springs, CA, Feb. 2010, pp. 2066–2072.
- 9 S. S. Raghavan, O. C. Onar, and A. Khaligh, "Power electronic interfaces for future plug-in transportation systems," *IEEE Power Electron. Soc. Newslett.*, vol. 24, no. 3, pp. 23–26, Third Quarter 2010.
- 10 Y.-J. Lee, A. Khaligh, and A. Emadi, "Advanced integrated bidirectional AC/DC and DC/DC converter for plug-in hybrid electric vehicles," *IEEE Trans. Veh. Technol.*, vol. 58, no. 5, pp. 3970–3980, Oct. 2009.
- 11 B. W. Williams, "Basic DC-to-DC converters," *IEEE Trans. Power Electron.*, vol. 23, no. 1, pp. 387–401, Jan. 2008.
- 12 B. Sahu and G. A. Rincon-Mora, "A low voltage, dynamic, noninverting, synchronous buck-boost converter for portable applications," *IEEE Trans. Power Electron.*, vol. 19, no. 2, pp. 443–452, Mar. 2004.
- 13 P. C. Huang, W. Q. Wu, H. H. Ho, and K. H. Chen, "Hybrid buck-boost feedforward and reduced average inductor current techniques in fast line transients and high-efficiency buck-boost converter," *IEEE Trans. Power Electron.*, vol. 25, no. 3, pp. 719–730, Mar. 2010.
- 14 S. Waffler and J. W. Kolar, "A novel low-loss modulation strategy for high-power bidirectional buck + boost converters," *IEEE Trans. Power Electron.*, vol. 24, no. 6, pp. 1589–1599, Jun. 2009.
- 15 M. B. Camara, H. Gualous, F. Gustin, A. Berthon, and B. Dakyo, "DC/DC converter design for supercapacitor and battery power management in hybrid vehicle

applications— Polynomial control strategy,” *IEEE Trans. Ind. Electron.*, vol. 57, no. 2, pp. 587–597, Feb. 2010.

16 M. C. Ghanem, K. Al-Haddad, and G. Roy, “A new control strategy to achieve sinusoidal line current in a cascade buck-boost converter,” *IEEE Trans. Ind. Electron.*, vol. 43, no. 3, pp. 441–449, Jun. 1996.

17 M. Gabriault and A. Notman, “A high efficiency, non-inverting, buckboost DC-DC converter,” in *Proc. IEEE 19th Annu. Appl. Power Electron. Conf. Expo.*, Anaheim, CA, Feb. 2004, vol. 3, pp. 1411–1415.

18 P. Midya, K. Haddad, and M. Miller, “Buck or boost tracking power controller,” *IEEE Trans. Power Electron.*, vol. 2, no. 4, pp. 131–134, Dec. 2004.

19 K. I. Hwu and Y. T. Yau, “Two types of KY buck-boost converters,” *IEEE Trans. Ind. Electron.*, vol. 56, no. 8, pp. 2970–2980, Aug. 2009.

20 D. Xu, C. Zhao, and H. Fan, “APWMplus phase-shift control bidirectional DC-DC converter,” *IEEE Trans. Power Electron.*, vol. 19, no. 3, pp. 666–675, May 2004.

21 M. Gang, L. Yuanyuan, and Q. Wenlong, “A novel soft switching bidirectional DC/DC converter and its output characteristics,” in *Proc. IEEE Region 10 Conf.*, Wan Chai, Hong Kong, Nov. 2006, pp. 1–4.

22 F. Krismer, J. Biela, and J. W. Kolar, “A comparative evaluation of isolated bi-directional DC/DC converters with wide input and output voltage range,” in *Proc. IEEE Ind. Appl. Conf.*, Kowloon, Hong Kong, Oct. 2005, vol. 1, pp. 599–606.

23 Y. Tsuruta, Y. Ito, and A. Kawamura, “Snubber-assisted zero-voltage and zero-current transition bilateral buck and boost chopper for EV drive application and test evaluation at 25 kW,” *IEEE Trans. Ind. Electron.*, vol. 56, no. 1, pp. 4–11, Jan. 2009.

24 D.-Y. Jung, S.-H. Hwang, Y.-H. Ji, J.-H. Lee, Y.-C. Jung, and C.-Y. Won, “Soft-switching bi-directional DC/DC converter with a LC series resonant circuit,” *IEEE Trans. Power Electron.*, vol. 28, no. 4, pp. 1680–1690, Apr. 2013.

25 H. Wu, J. Lu, W. Shi, and Y. Xing, “Nonisolated bidirectional DC-DC converters with negative coupled inductor,” *IEEE Trans. Power Electron.*, vol. 27, no. 5, pp. 2231–2235, May 2012.

26 H.-L. Do, “Nonisolated bidirectional zero-voltage-switching DC-DC converter,” *IEEE Trans. Power Electron.*, vol. 26, no. 9, pp. 2563–2569, Sep. 2011.

27 L. Ni, D. J. Patterson, and J. L. Hudgins, “High power current sensorless bidirectional 16-phase interleaved DC-DC converter for hybrid vehicle application,” *IEEE Trans. Power Electron.*, vol. 27, no. 3, pp. 1141–1151, Mar. 2012.

AUTHOR’S PROFILE



Mandadi Sagar Reddy received the B.Tech degree in Electrical and Electronics Engineering from Netaji institute of Engineering & technology, India in 2011 and at present Pursuing M.Tech with the Specialization of Power Electronics and Electric Drives in Anurag Engineering college Kodad.



D. Pomya graduated in EEE from Anurag Engineering College in 2007. He received M.E degree in the stream of Power Electronics in Osmania University in 2009, presently working as Assistant Professor in Anurag Engineering college.